

# Directed Weight Neural Networks for Protein Structure Representation Learning

## Abstract

A protein performs biological functions by folding to a particular 3D structure. To accurately model the protein structures, both the overall geometric topology and local fine-grained relations between amino acids (e.g. side-chain torsion angles and inter-amino-acid orientations) should be carefully considered. In this work, we propose the Directed Weight Neural Network for better capturing geometric relations among different amino acids. Extending a single weight from a scalar to a 3D directed vector, our new framework supports a rich set of geometric operations on both classical and SO(3)-representation features, on top of which we construct a perceptron unit for processing amino-acid information. In addition, we introduce an equivariant message passing paradigm on proteins for plugging the directed weight perceptrons into existing Graph Neural Networks, showing superior versatility in maintaining SO(3)-equivariance at the global scale. Experiments show that our network has remarkably better expressiveness in representing geometric relations in comparison to classical neural networks and the (globally) equivariant networks. It also achieves state-of-the-art performance on various computational biology applications related to protein 3D structures. All codes and models will be published upon acceptance.

## 1. Introduction

Built from a sequence of amino acid residues, a protein performs its biological functions by folding to a particular 3D conformation. Therefore, processing such 3D structures is the key for protein function analysis. While we have witnessed remarkable progress in protein structure predictions (Rohl et al., 2004; Källberg et al., 2012; Baek et al., 2021; Jumper et al., 2021), another thread of tasks with protein 3D structures as input starts to draw a great interest, such as function prediction (Hermosilla et al., 2020; Gligorijević

et al., 2021), decoy ranking (Lundström et al., 2001; Kwon et al., 2021; Wang et al., 2021), protein docking (Duhovny et al., 2002; Shulman-Peleg et al., 2004; Gainza et al., 2020; Sverrisson et al., 2021), and driver mutation identification (Lefèvre et al., 1997; Antikainen & Martin, 2005; Li et al., 2020; Jankauskaitė et al., 2019).

Most existing works in modelling protein structures directly borrow neural network designs from other application areas such as computer vision and data mining (e.g. 3D-CNNs (Ji et al., 2012), GNNs (Kipf & Welling, 2016), Transformers (Vaswani et al., 2017)). Although compatible with general 3D object data, these models mainly focus on the overall protein topology but overlook the subtleties in the fine-grained geometries, which could be essential in many scenarios. For instance, given an amino acid characterized by its backbone atoms (carbon, nitrogen, and oxygen) and a side-chain, as shown in Figure 1, the locations of the backbone atoms determine the protein skeleton locally and its local frame orientation affects how it interacts with other amino acids, either of which can have important impacts on the entire protein structure (Nelson et al., 2008). It is also well-known that a small change to the side chain angles could cause a significant change to the protein functionality, especially when it interacts with other biological molecules (Jacobson et al., 2002; Misiura et al., 2021).

Recent attempts in building geometric-aware neural networks mainly focus on baking 3D *rigid transformations* into network operations, leading to the area of SO(3)-invariant and equivariant networks. One of representative works is the Vector Neuron Network (VNN) (Deng et al., 2021), which achieves SO(3)-equivariance on point clouds by generalizing scalar neurons to vectors. Another follow-up work is the GVP-GNN (Jing et al., 2021) that similarly vectorizes hidden neurons on GNN and demonstrates better prediction accuracy on protein design and quality evaluation tasks. These models adopt *linear combinations* of input vector features, which significantly limits their modeling capability. A simple example is that, given two input vector features  $v_1$  and  $v_2$ , the outputs  $w_1v_1 + w_2v_2$  through one linear layer is constrained in the 2D plane spanned by  $v_1, v_2$  even after applying their vector version of non-linearities. A more concrete application in the experiment section demonstrates how VNN-based models are limited in perceiving angles

<sup>\*</sup>Equal contribution .  
\icmlcorrespondingauthor.

AUTHORERR: Missing

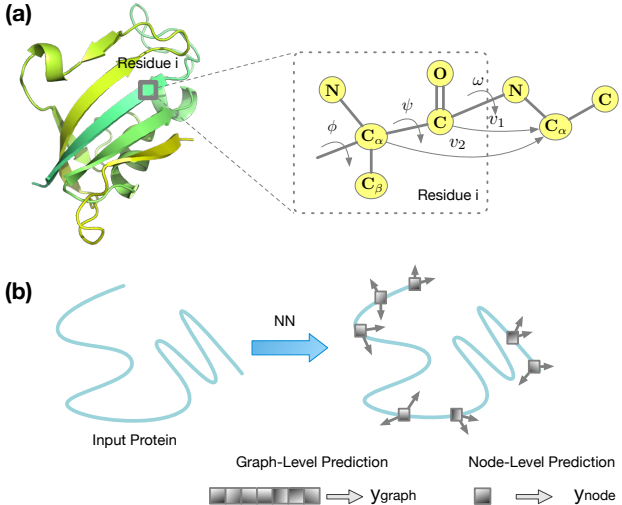


**Figure 1.** Overview. a). Each amino acid has its own **rigid backbone** with four heavy atoms, and can be represented by both lists of scalar and vector features. b). Protein representation tasks associated with the 3D structure. **Graph-level** tasks evaluate the whole protein structures, and **Node-level** tasks operates on each residues

(e.g. side-chain torsion angles), which have been proven crucial for proteins to interact with other partners through non-covalent bonds (Nelson et al., 2008).

To achieve more sensitive geometric awareness in both global transformations and local relations, we propose a *Directed Weight* ( $\bar{W}$ ) *perceptrons* by extending not only the hidden neurons but the weights from scalars to 2D/3D vectors, naturally saturating the entire network with 3D structures in the Euclidean space. Directed weights support a set of geometric operations on both the vector neurons (vector-list features) and the classical (scalar-list) latent features, and perform flexible integration of the hybrid scalar-vector features. As protein structures are naturally attributed proximity graphs, we introduce a new *Equivariant Message Passing Paradigm* on protein graphs, to connect the  $\bar{W}$ -perceptrons with the graph learning models by using rigid backbone transformations for each amino acid, which provides a versatile framework for bringing the biological suitability and flexibility of the GNN architecture. This paradigm frees the model architecture itself from introducing additional equivariance constraints (Cohen & Welling, 2016), making more complicated model designs possible.

To summarize, our key contributions include:

- We propose a new learning framework based on the *Directed Weights* for capturing fine-grained geometric relations, especially for the subtle structure details in proteins.
- We construct an *Equivariant Message Passing* paradigm based on protein structures.
- Our overall framework is versatile in terms of com-

patibility with existing deep graph learning models, making them biologically suitable with minimal modifications of existing GNN models.

- We demonstrate our network expressivity over classical scalar-weighted networks on a synthetic dataset. Our models also achieve state-of-the-art performance on multiple protein learning tasks.

## 2. Related Work

**Representation learning on protein 3D structure.** Using machine learning models to understand protein 3D structures could be traced back to a decade ago. Early approaches mainly rely on hand-crafted features extracted from protein structures and simple statistical methods are adopted to predict multiple functional annotations (Schaap et al., 2001; Zhang & Zhang, 2010). Later, deep learning models have been found to achieve tremendous success in this area. 3D CNNs are first proposed to process protein 3D structures by scanning atom-level features relying on multiple 3D voxels. One of the representative works by Derevyanko et al. (2018) adopts a 3D CNN-based model for assessing the quality of the predicted structures and achieves state-of-the-art performance. Amidi et al. (2018) employs a similar idea to classify enzymes classes by using 3D CNN. 3D CNNs also shed light on other tasks such as interface prediction (Townshend et al., 2019) and protein fold recognition (Hermosilla et al., 2020). Gainza et al. (2020); Sverrisson et al. (2021) extend 3D CNNs to spherical convolutions for operating on radius regions, which can also be naturally applied to the Fourier space (Zhemchuzhnikov et al., 2021) and the 3D Voronoi Tessellation space (Igashov et al., 2021). Graph Convolutional Networks have also been adopted to capture geometric relationships and biochemical interactions between amino acids in the protein structures (Ying et al., 2018; Gao & Ji, 2019; Fout, 2017), and have been shown to achieve tremendous success in protein function prediction (Li et al., 2021), protein design (Strokach et al., 2020) and binding affinity/site prediction (Vecchio et al., 2021). More recently, transformer-based methods have drawn a lot of interest in extracting representations for protein structures and have a trend to replace conventional 3D CNN-based methods in other bioinformatics tasks (Ingraham et al., 2019; Baek et al., 2021; Jumper et al., 2021; Cao et al., 2021).

**Equivariant neural networks.** Equivariance is an important property for geometric learning models to generalize to unseen conditions (Cohen & Welling, 2016; Weiler et al., 2018; Köhler et al., 2020; Satorras et al., 2021; Thomas et al., 2018; Fuchs et al., 2020; Anderson et al., 2019; Klicpera et al., 2020; Batzner et al., 2021; Eismann et al., 2021). While data augmentation is not an appropriate solution, neural network models such as Tensor Filed Network (Thomas et al., 2018) and Cormorant (Anderson et al., 2019), have

been developed to generate irreducible representations for achieving rotation equivariant for 3D objects. In comparison to Tensor Filed Network and Cormorant, the vector neuron network (VNN) achieves rotation equivariance in a much simpler way by generalizing the values of hidden neurons from scalars to vectors defined in the 3D Euclidean space (Deng et al., 2021). Jing et al. (2020) later introduces GVP-GNN for learning protein structure representations by considering geometric factors such as orientations as vector representations and gains reasonable performance improvement on downstream tasks. Schütt et al. (2021) introduces equivariant message passing for vector representations using equivariant features. However, to guarantee rotation equivariance, these vector-based networks can only linearly combine 3D vectors, in essence, limiting their geometric expressiveness.

### 3. Directed Weight Perceptron

A protein is modeled as a KNN-graph  $\mathcal{G} = (\mathcal{V}, \mathcal{E})$  where each node  $u \in \mathcal{V}$  corresponds to one amino acid represented by a scalar-vector tuple  $h_u = (s_u, \mathbf{V}_u)$  with  $s_u \in \mathbb{R}^C$ ,  $\mathbf{V}_u \in \mathbb{R}^{C \times 3}$ , and the edges are constructed spatially by querying its  $k$ -nearest neighbours in the space. For notation simplicity, we set the channel numbers for scalar and vector features as the same but they can be different in practice. Details for the channel numbers can be found in the appendix Section B.1.

Classical neural networks only consider scalar features of the form  $s \in \mathbb{R}^C$ , with each layer transforming them with a weight matrix  $\mathbf{W} \in \mathbb{R}^{C' \times C}$  and a bias term  $\mathbf{b} \in \mathbb{R}^{C'}$ :

$$s' = \mathbf{W}s + \mathbf{b} \quad (1)$$

Although has been proved to be a universal approximator, such layer has intrinsically no geometric interpretation in the 3D shape space, limiting both expressiveness and robustness – even a simplest 3D rigid transformation on the input can result in drastic and unpredictable changes in the network outputs. Recent attempts studying equivariance (Deng et al., 2021; Jing et al., 2020) have lifted neuron features from scalar-lists to vector-lists  $\mathbf{V} \in \mathbb{R}^{C \times 3}$  with a layer operation:

$$\mathbf{V}' = \mathbf{W}\mathbf{V} \quad (2)$$

Under this construction, latent space  $\text{SO}(3)$ -actions are simply matrix (right) multiplications, which establishes a clear 3D Euclidean structure on the latent space and shows input-output consistency under rigid transformations. Despite the vectorization of features and their hidden representations, their operations are still limited to classical linear combinations weighted by  $\mathbf{W}$ . To define *operations* that are more adaptive to the geometrically meaningful features, we introduce the *Directed Weights*, denoted by  $\vec{\mathbf{W}} \in \mathbb{R}^{C' \times C \times 3}$ , accompanied with a set of geometric operators  $\square$  (e.g.  $\cdot$

or  $\times$ ) on both scalar-list features  $s \in \mathbb{R}^C$  and vector-list features  $\mathbf{V} \in \mathbb{R}^{C \times 3}$

$$\vec{\mathbf{W}} \square s, \quad \vec{\mathbf{W}} \square \mathbf{V} \quad (3)$$

, allowing flexible architectural designs with rich expressiveness in geometric relations.

#### 3.1. $\vec{\mathbf{W}}$ -Operators

**Geometric Vector Operations.** Let  $\mathbf{W} \in \mathbb{R}^{C' \times C}$  be a conventional scalar weight matrix,  $\vec{\mathbf{W}}_1 \in \mathbb{R}^{C' \times C \times 3}$  and  $\vec{\mathbf{W}}_2 \in \mathbb{R}^{C \times 3}$  be directed weight tensors. We can define two operations that leverage geometric information:

$$s'_{\text{dot}}(\mathbf{V}; \vec{\mathbf{W}}_1) = \vec{\mathbf{W}}_1 \mathbf{V} \quad \in \mathbb{R}^{C'} \quad (4)$$

$$\mathbf{V}'_{\text{crs}}(\mathbf{V}; \vec{\mathbf{W}}_1, \vec{\mathbf{W}}_2) = \vec{\mathbf{W}}_1 \cdot (\vec{\mathbf{W}}_2 \times \mathbf{V}) \quad \in \mathbb{R}^{C' \times 3} \quad (5)$$

Here  $s'_{\text{dot}}$  transforms  $C$  vector features to  $C'$  scalars using dot-product with directed weights, which explicitly measures angles between vectors. In  $\mathbf{V}'_{\text{crs}}$ , a vector crosses a directed weight before being projected onto the hidden space. As the output of plain linear combinations between two vectors  $\mathbf{v}_1$  and  $\mathbf{v}_2$  can only lie in the plane  $w_1\mathbf{v}_1 + w_2\mathbf{v}_2$ , cross-product in Equation 5 creates a new direction outside the plane, which is crucial in 3D modelling. For instance, the side-chain angles of a given residue could be largely determined by its  $C_\alpha$  and  $C_\beta$  vectors, but may lie on the direction perpendicular to the space constructed by the two vectors.

**Scalar Lifting.** In addition, a directed weight  $\vec{\mathbf{W}} \in \mathbb{R}^{C \times 3}$  can lift scalars to vectors by adopting the following operation,

$$\mathbf{V}'_{\text{lift}}(s; \vec{\mathbf{W}}) = s \vec{\mathbf{W}} \quad \in \mathbb{R}^{C \times 3} \quad (6)$$

This maps each scalar to a particular vector, enabling inverse transformations from  $\mathbb{R}$  to  $\mathbb{R}^3$ . For instance, we can map a scalar representing the distance between two amino acids to a vector pointing from one amino acid to the other, leading to more biologically meaningful representations for the protein fragment.

**Linear Combinations.** In the end, we keep the linear combination operations with scalar weights for both scalar and vector features:

$$s'_{\text{lin}}(s; \mathbf{W}) = \mathbf{W}s \quad \in \mathbb{R}^{C'} \quad (7)$$

$$\mathbf{V}'_{\text{lin}}(\mathbf{V}; \mathbf{W}) = \mathbf{W}\mathbf{V} \quad \in \mathbb{R}^{C' \times 3} \quad (8)$$

#### 3.2. $\vec{\mathbf{W}}$ -Perceptron Unit

Now we combine all the  $\vec{\mathbf{W}}$ -operators together, assembling them into what we call Directed Weight Perceptrons ( $\vec{\mathbf{W}}$ -perceptrons) for processing the protein 3D structures. A

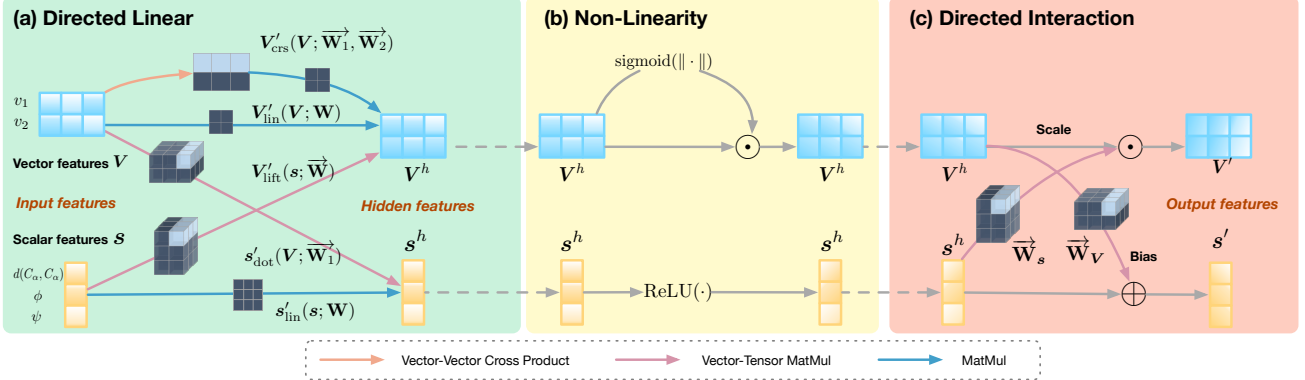


Figure 2. Model Details. a) **Directed Linear Module** applies multiple geometric operations to update scalar and vector features respectively. b) **Non-Linearity Modules** employs ReLU and sigmoid functions for scalar and vector representations. c) **Directed Interaction Module** updates the features by using one another as updating parameters.

$\overrightarrow{\mathbf{W}}$ -perceptron unit is a function mapping from  $u = (s, \mathbf{V})$  to another scalar-vector tuple  $u' = (s', \mathbf{V}')$ , which can be stacked as network layers to form multi-layer perceptrons.

A single unit comprises three modules in a sequential way: the **Directed Linear** module, the **Non-Linearity** module, and the **Directed Interaction** module (Figure 2). We show that these modules can properly tackle the defects of prior models and encourage efficient scalar-vector feature interactions within the network.

**Directed Linear Module.** The output hidden representations derived from the set of operations introduced previously are concatenated and projected into another hidden space of scalars and vectors separately:

$$s^h = \mathbf{W}_s[s'_{\text{dot}}, s'_{\text{lin}}] \in \mathbb{R}^{C'} \quad (9)$$

$$\mathbf{V}^h = \mathbf{W}_V[V'_{\text{crs}}, V'_{\text{lift}}, V'_{\text{lin}}] \in \mathbb{R}^{C' \times 3} \quad (10)$$

Here  $\mathbf{W}_s \in \mathbb{R}^{C' \times (C'+C')}$  and  $\mathbf{W}_V \in \mathbb{R}^{C' \times (C'+C+C')}$  are scalar weight matrices. In other word, the five separate updating functions allow transformation from scalar to scalar (Equation 7), scalar to vector (Equation 6), vector to scalar (Equation 4), and vector to vector (Equation 8, Equation 5), , boosting the model’s expressiveness to reason geometrically.

**Non-linearity Module.** We then apply the non-linearity module to the hidden representation  $(s^h, \mathbf{V}^h)$ . Specifically, we apply standard ReLU non-linearity (Nair & Hinton, 2010) to the scalar components. For the vector representations, following (Weiler et al., 2018; Jing et al., 2020; Schütt et al., 2021), we compute a sigmoid activation on the L2-norm of each vector and multiply it back to the vector entries accordingly:

$$s^h \leftarrow \text{ReLU}(s^h) \quad (11)$$

$$v_{ij}^h \leftarrow v_{ij}^h \cdot \text{sigmoid}(\|\mathbf{v}_i^h\|_2) \quad (12)$$

where  $\mathbf{v}_i^h \in \mathbb{R}^3$  are the vector columns in  $\mathbf{V}^h$  and  $v_{ij}^h$  are their entries.

**Directed Interaction Module.** Finally we introduce the Directed Interaction module, integrating the hidden features  $s^h$  and  $\mathbf{V}^h$  into the output tuple  $(s', \mathbf{V}')$

$$s' = s^h + \overrightarrow{\mathbf{W}}_V \cdot \mathbf{V}^h \in \mathbb{R}^{C'} \quad (13)$$

$$\mathbf{V}' = (s^h \overrightarrow{\mathbf{W}}_s) \odot \mathbf{V}^h \in \mathbb{R}^{C' \times 3} \quad (14)$$

Here  $\overrightarrow{\mathbf{W}}_V, \overrightarrow{\mathbf{W}}_s$  are directed weight matrices with sizes  $C' \times C' \times 3$  and  $C' \times 3$ , respectively,  $\odot$  denotes element-wise multiplication for two matrices. This module establishes a connection between the scalar and vector feature components, facilitating feature blending. Specifically, Equation 13 dynamically determines how much the output should rely on scalar and vector representations, and Equation 14 weights a list of vectors using the scalar features as attention scores.

## 4. $\overrightarrow{\mathbf{W}}$ -Equivariant Graph Neural Networks

Conventional message-passing-based graph neural networks (Gilmer et al., 2017; Thomas et al., 2018) for molecular modeling do not allow scalar-vector communications and usually treat them as separate channels. While being versatile enough to be plugged into any existing message passing networks, our  $\overrightarrow{\mathbf{W}}$ -Perceptron also provides a more flexible toolbox bridging scalar and vector channels with geometrical and biological interpretations. On the other hand, to achieve SO(3)-equivariance without the loss of expressivity, we introduce an equivariant message passing paradigm for protein graphs, making network architecture designs free from the geometric constraints (Section 4.1). In the end, we demonstrate our adaptability by integrating this framework into multiple graph neural networks variants (Section 4.2).

#### 4.1. Equivariant Message Passing on Proteins

A function  $f : \mathbb{R}^3 \rightarrow \mathbb{R}^3$  is  $\text{SO}(3)$ -equivariant (rotation-equivariant) if any rotation matrix  $R \in \mathbb{R}^{3 \times 3}$  applied to the input vector  $x$  leads to the same transformation on the output  $f(x)$ :

$$Rf(x) = f(Rx) \quad (15)$$

Such equivariant property can be achieved on a protein graph with local orientations naturally defined from its biological structure. Specifically, each amino acid node  $u_i \in \mathcal{V}$  has four backbone heavy atom ( $C_\alpha^u, C_\beta^u, N^u, O^u$ ), defining a local frame  $\mathbf{O}_u$  as:

$$\mathbf{x}_u = N^u - C_\alpha^u \in \mathbb{R}^3 \quad (16)$$

$$\mathbf{y}_u = C_\beta^u - C_\alpha^u \in \mathbb{R}^3 \quad (17)$$

$$\mathbf{O}_u = [\mathbf{x}_u, \mathbf{y}_u, \mathbf{x}_u \times \mathbf{y}_u]^\top \in \mathbb{R}^{3 \times 3} \quad (18)$$

The local frame  $\mathbf{O}_u$  is a rotation matrix that maps a 3D vector from the local to the global coordinate system. An equivariant message passing paradigm then emerges through transforming node features back and forth between adjacent local frames. Formally, give an amino acid  $u$  with hidden representation  $h = (\mathbf{s}, \mathbf{V})$ , let  $f_l$  and  $f_g$  be transformations on the vector feature  $\mathbf{V}$  from and to the global coordinate system:

$$f_l(h, \mathbf{O}_u) := (\mathbf{s}, \mathbf{V}\mathbf{O}_u^\top) \quad (19)$$

$$f_g(h, \mathbf{O}_u) := (\mathbf{s}, \mathbf{V}\mathbf{O}_u) \quad (20)$$

The message passing update for node  $u$  from layer  $l$  to layer  $l+1$  is performed in the following steps:

1. Transform the neighbourhood vector representations of  $u$  into its local coordinate system  $\mathbf{O}_u$ .
2. For each adjacent node  $v$ , compute the message  $m_u^{l+1}$  on edge  $(u, v) \in \mathcal{E}$  with a multi-layer  $\vec{\mathbf{W}}$ -perceptron  $\mathcal{F}$  to the aggregated node and edge feature  $[h_u^l, h_v^l, e_{uv}^l]$  (Equation 21).
3. Update node feature  $h_u^l$  with another multi-layer  $\vec{\mathbf{W}}$ -perceptron  $\mathcal{H}$ , and transform it back to the global coordinate system (Equation 22).

This paradigm achieves  $\text{SO}(3)$ -equivariance in a very general sense with no constraints on  $\mathcal{F}, \mathcal{H}$ . The formal proof of equivariance is presented in the appendix Section A.

$$m_u^{l+1} = \sum_{v \in \mathcal{N}_u} \mathcal{F}(f_l([h_u^l, h_v^l, e_{uv}^l], \mathbf{O}_u)) \quad (21)$$

$$h_u^{l+1} = f_g(\mathcal{H}(h_u^l, m_u^{l+1}), \mathbf{O}_u) \quad (22)$$

#### 4.2. $\vec{\mathbf{W}}$ -Graph Neural Networks

Different variants of GNN models have been demonstrated to be helpful for different bioinformatics tasks involving

protein 3D structures (Ingraham et al., 2019; Strokach et al., 2020; Baldassarre et al., 2021). Therefore, we integrate the  $\vec{\mathbf{W}}$ -Perceptrons with our proposed equivariant message passing paradigm into multiple popular GNN frameworks.

**DW-GCN.** This is the one described and implemented in the previous subsection with Equation 21 and Equation 22.

**DW-GIN.** We adopt graph isomorphism operator (Xu et al., 2018) with learnable weighing parameter  $\varepsilon$  for tunable skip connections,

$$m_u^{l+1} = (1 + \varepsilon)f_l(h_u^l, \mathbf{O}_u) + \sum_{v \in \mathcal{N}_u} \mathcal{F}(f_l(h_v^l, \mathbf{O}_u)) \quad (23)$$

**DW-GAT.** In comparison to GCN and GIN, it is not trivial to incorporate with the Graph Attention Network (GAT) (Veličković et al., 2017). In particular, we define separate attentions for the scalar and vector representations

$$(\mathbf{s}_u^l, \mathbf{V}_u^l) = f_l(h_u^l, \mathbf{O}_u) \quad (24)$$

$$\mathbf{s}'_u = \sum_{v \in \mathcal{N}_u \cup \{u\}} \alpha_v^s \mathbf{s}_v^l \quad (25)$$

$$\mathbf{V}'_u = \sum_{v \in \mathcal{N}_u \cup \{u\}} \alpha_v^v \mathbf{V}_v^l \quad (26)$$

$$h_u^{l+1} = f_g(\mathcal{H}((\mathbf{s}', \mathbf{V}'), \mathbf{O}_u)) \quad (27)$$

The attention scores  $\alpha^s, \alpha^v$  are the softmax values over the inner products of all neighboring source-target pairs defined as the follows:

$$\alpha_v^s = \frac{\exp(\langle \mathbf{s}_u, \mathbf{s}_v \rangle)}{\sum_{w \in \mathcal{N}_u \cup \{u\}} \exp(\langle \mathbf{s}_u, \mathbf{s}_w \rangle)} \quad (28)$$

$$\alpha_v^v = \frac{\exp(\text{tr}(\mathbf{V}_u^\top \mathbf{V}_v))}{\sum_{w \in \mathcal{N}_u \cup \{u\}} \exp(\text{tr}(\mathbf{V}_u^\top \mathbf{V}_w))} \quad (29)$$

The product for scalars and vectors are standard inner product (Equation 28) and Frobenius product (Equation 29), respectively. With the attention mechanism, an amino acid can determine the subset of neighbors which contribute more to obtain representations, as amino acids interact with each other unevenly.

## 5. Conclusion

For the first time, we generalize the scalar weights in neural networks to 3D directed vectors for better perception of geometric features like orientations and angles, which are essential in learning representations from protein 3D structures. Based on the directed weights  $\vec{\mathbf{W}}$ , we provide a toolbox of operators as well as a  $\vec{\mathbf{W}}$ -Perceptron Unit encouraging efficient scalar-vector feature interactions. We also enforce global  $\text{SO}(3)$ -equivariance on a message passing paradigm using the local orientations naturally defined by the rigid property of each amino acid residue, which can be

used for designing more powerful networks. Our  $\vec{W}$  versions of popular graph neural network architectures achieve comparably good or better performances on multiple biological tasks in comparison with existing state-of-the-art methods.

**Limitations and future work.** While our methods show great performance, there is still a huge design space of Non-Linearity functions for SO(3) vector representations. In the future, we will extend our framework to other 3D learning tasks like small molecules or point clouds by learning local rotation transformations and using directed vector weights.

## References

- Amidi, A., Amidi, S., Vlachakis, D., Megalooikonomou, V., Paragios, N., and Zacharaki, E. I. Enzynet: enzyme classification using 3d convolutional neural networks on spatial representation. *PeerJ*, 6:e4750, 2018.
- Anderson, B., Hy, T.-S., and Kondor, R. Cormorant: Covariant molecular neural networks. *arXiv preprint arXiv:1906.04015*, 2019.
- Antikainen, N. M. and Martin, S. F. Altering protein specificity: techniques and applications. *Bioorganic & medicinal chemistry*, 13(8):2701–2716, 2005.
- Baek, M., DiMaio, F., Anishchenko, I., Dauparas, J., Ovchinnikov, S., Lee, G. R., Wang, J., Cong, Q., Kinch, L. N., Schaeffer, R. D., et al. Accurate prediction of protein structures and interactions using a three-track neural network. *Science*, 373(6557):871–876, 2021.
- Baldassarre, F., Menéndez Hurtado, D., Elofsson, A., and Azizpour, H. Graphqa: protein model quality assessment using graph convolutional networks. *Bioinformatics*, 37(3):360–366, 2021.
- Batzner, S., Smidt, T. E., Sun, L., Mailoa, J. P., Kornbluth, M., Molinari, N., and Kozinsky, B. Se (3)-equivariant graph neural networks for data-efficient and accurate interatomic potentials. *arXiv preprint arXiv:2101.03164*, 2021.
- Cao, Y., Das, P., Chenthamarakshan, V., Chen, P.-Y., Melnyk, I., and Shen, Y. Fold2seq: A joint sequence (1d)-fold (3d) embedding-based generative model for protein design. In *International Conference on Machine Learning*, pp. 1261–1271. PMLR, 2021.
- Cohen, T. and Welling, M. Group equivariant convolutional networks. In *International conference on machine learning*, pp. 2990–2999. PMLR, 2016.
- Deng, C., Litany, O., Duan, Y., Poulenard, A., Tagliasacchi, A., and Guibas, L. Vector neurons: A general framework for so (3)-equivariant networks. *arXiv preprint arXiv:2104.12229*, 2021.
- Derevyanko, G., Grudinin, S., Bengio, Y., and Lamoureux, G. Deep convolutional networks for quality assessment of protein folds. *Bioinformatics*, 34(23):4046–4053, 2018.
- Duhovny, D., Nussinov, R., and Wolfson, H. J. Efficient unbound docking of rigid molecules. In *International workshop on algorithms in bioinformatics*, pp. 185–200. Springer, 2002.
- Eismann, S., Townshend, R. J., Thomas, N., Jagota, M., Jing, B., and Dror, R. O. Hierarchical, rotation-equivariant neural networks to select structural models of protein complexes. *Proteins: Structure, Function, and Bioinformatics*, 89(5):493–501, 2021.
- Fout, A. M. *Protein interface prediction using graph convolutional networks*. PhD thesis, Colorado State University, 2017.
- Fuchs, F. B., Worrall, D. E., Fischer, V., and Welling, M. Se (3)-transformers: 3d roto-translation equivariant attention networks. *arXiv preprint arXiv:2006.10503*, 2020.
- Gainza, P., Svärrisson, F., Monti, F., Rodola, E., Boscaini, D., Bronstein, M., and Correia, B. Deciphering interaction fingerprints from protein molecular surfaces using geometric deep learning. *Nature Methods*, 17(2):184–192, 2020.
- Gao, H. and Ji, S. Graph u-nets. In *international conference on machine learning*, pp. 2083–2092. PMLR, 2019.
- Gilmer, J., Schoenholz, S. S., Riley, P. F., Vinyals, O., and Dahl, G. E. Neural message passing for quantum chemistry. In *International conference on machine learning*, pp. 1263–1272. PMLR, 2017.
- Gligorjević, V., Renfrew, P. D., Kosciolak, T., Leman, J. K., Berenberg, D., Vatanen, T., Chandler, C., Taylor, B. C., Fisk, I. M., Vlamakis, H., et al. Structure-based protein function prediction using graph convolutional networks. *Nature communications*, 12(1):1–14, 2021.
- Hermosilla, P., Schäfer, M., Lang, M., Fackelmann, G., Vázquez, P. P., Kozlíková, B., Krone, M., Ritschel, T., and Ropinski, T. Intrinsic-extrinsic convolution and pooling for learning on 3d protein structures. *arXiv preprint arXiv:2007.06252*, 2020.
- Igashov, I., Olechnovič, K., Kadukova, M., Venclovas, Č., and Grudinin, S. Vorocnn: deep convolutional neural network built on 3d voronoi tessellation of protein structures. *Bioinformatics*, 37(16):2332–2339, 2021.
- Ingraham, J., Garg, V. K., Barzilay, R., and Jaakkola, T. Generative models for graph-based protein design. 2019.

- Jacobson, M. P., Friesner, R. A., Xiang, Z., and Honig, B. On the role of the crystal environment in determining protein side-chain conformations. *Journal of molecular biology*, 320(3):597–608, 2002.
- Jankauskaitė, J., Jiménez-García, B., Dapkūnas, J., Fernández-Recio, J., and Moal, I. H. Skempi 2.0: an updated benchmark of changes in protein–protein binding energy, kinetics and thermodynamics upon mutation. *Bioinformatics*, 35(3):462–469, 2019.
- Ji, S., Xu, W., Yang, M., and Yu, K. 3d convolutional neural networks for human action recognition. *IEEE transactions on pattern analysis and machine intelligence*, 35(1):221–231, 2012.
- Jing, B., Eismann, S., Suriana, P., Townshend, R. J., and Dror, R. Learning from protein structure with geometric vector perceptrons. *arXiv preprint arXiv:2009.01411*, 2020.
- Jing, B., Eismann, S., Soni, P. N., and Dror, R. O. Equivariant graph neural networks for 3d macromolecular structure. *arXiv preprint arXiv:2106.03843*, 2021.
- Jumper, J., Evans, R., Pritzel, A., Green, T., Figurnov, M., Ronneberger, O., Tunyasuvunakool, K., Bates, R., Žídek, A., Potapenko, A., et al. Highly accurate protein structure prediction with alphafold. *Nature*, 596(7873):583–589, 2021.
- Källberg, M., Wang, H., Wang, S., Peng, J., Wang, Z., Lu, H., and Xu, J. Template-based protein structure modeling using the raptord web server. *Nature protocols*, 7(8):1511–1522, 2012.
- Kipf, T. N. and Welling, M. Semi-supervised classification with graph convolutional networks. *arXiv preprint arXiv:1609.02907*, 2016.
- Klicpera, J., Groß, J., and Günnemann, S. Directional message passing for molecular graphs. *arXiv preprint arXiv:2003.03123*, 2020.
- Köhler, J., Klein, L., and Noé, F. Equivariant flows: exact likelihood generative learning for symmetric densities. In *International Conference on Machine Learning*, pp. 5361–5370. PMLR, 2020.
- Kwon, S., Won, J., Kryshtafovych, A., and Seok, C. Assessment of protein model structure accuracy estimation in casp14: Old and new challenges. *Proteins: Structure, Function, and Bioinformatics*, 2021.
- Lefèvre, F., Rémy, M.-H., and Masson, J.-M. Alanine-stretch scanning mutagenesis: a simple and efficient method to probe protein structure and function. *Nucleic acids research*, 25(2):447–448, 1997.
- Li, B., Yang, Y. T., Capra, J. A., and Gerstein, M. B. Predicting changes in protein thermodynamic stability upon point mutation with deep 3d convolutional neural networks. *bioRxiv*, 2020. doi: 10.1101/2020.02.28.959874.
- Li, S., Zhou, J., Xu, T., Huang, L., Wang, F., Xiong, H., Huang, W., Dou, D., and Xiong, H. Structure-aware interactive graph neural networks for the prediction of protein-ligand binding affinity. In *Proceedings of the 27th ACM SIGKDD Conference on Knowledge Discovery & Data Mining*, pp. 975–985, 2021.
- Lundström, J., Rychlewski, L., Bujnicki, J., and Elofsson, A. Pcons: A neural-network-based consensus predictor that improves fold recognition. *Protein science*, 10(11):2354–2362, 2001.
- Misiura, M., Shroff, R., Thyer, R., and Kolomeisky, A. Dlpacker: Deep learning for prediction of amino acid side chain conformations in proteins. *bioRxiv*, 2021.
- Nair, V. and Hinton, G. E. Rectified linear units improve restricted boltzmann machines. In *Icml*, 2010.
- Nelson, D. L., Lehninger, A. L., and Cox, M. M. *Lehninger principles of biochemistry*. Macmillan, 2008.
- Rohr, C. A., Strauss, C. E., Misura, K. M., and Baker, D. Protein structure prediction using rosetta. *Methods in enzymology*, 383:66–93, 2004.
- Satorras, V. G., Hoogeboom, E., and Welling, M. E (n) equivariant graph neural networks. *arXiv preprint arXiv:2102.09844*, 2021.
- Schaap, M. G., Leij, F. J., and Van Genuchten, M. T. Rosetta: A computer program for estimating soil hydraulic parameters with hierarchical pedotransfer functions. *Journal of hydrology*, 251(3-4):163–176, 2001.
- Schütt, K. T., Unke, O. T., and Gastegger, M. Equivariant message passing for the prediction of tensorial properties and molecular spectra. *arXiv preprint arXiv:2102.03150*, 2021.
- Shulman-Peleg, A., Nussinov, R., and Wolfson, H. J. Recognition of functional sites in protein structures. *Journal of molecular biology*, 339(3):607–633, 2004.
- Srivastava, N., Hinton, G., Krizhevsky, A., Sutskever, I., and Salakhutdinov, R. Dropout: a simple way to prevent neural networks from overfitting. *The journal of machine learning research*, 15(1):1929–1958, 2014.
- Strokach, A., Becerra, D., Corbi-Verge, C., Perez-Riba, A., and Kim, P. M. Fast and flexible protein design using deep graph neural networks. *Cell Systems*, 11(4):402–411, 2020.

Sverrisson, F., Feydy, J., Correia, B. E., and Bronstein, M. M. Fast end-to-end learning on protein surfaces. In *Proceedings of the IEEE/CVF Conference on Computer Vision and Pattern Recognition*, pp. 15272–15281, 2021.

Thomas, N., Smidt, T., Kearnes, S., Yang, L., Li, L., Kohlhoff, K., and Riley, P. Tensor field networks: Rotation-and translation-equivariant neural networks for 3d point clouds. *arXiv preprint arXiv:1802.08219*, 2018.

Townshend, R., Bedi, R., Suriana, P., and Dror, R. End-to-end learning on 3d protein structure for interface prediction. *Advances in Neural Information Processing Systems*, 32:15642–15651, 2019.

Vaswani, A., Shazeer, N., Parmar, N., Uszkoreit, J., Jones, L., Gomez, A. N., Kaiser, Ł., and Polosukhin, I. Attention is all you need. In *Advances in neural information processing systems*, pp. 5998–6008, 2017.

Vecchio, A., Deac, A., Liò, P., and Veličković, P. Neural message passing for joint paratope-epitope prediction. 2021.

Veličković, P., Cucurull, G., Casanova, A., Romero, A., Lio, P., and Bengio, Y. Graph attention networks. *arXiv preprint arXiv:1710.10903*, 2017.

Wang, X., Flannery, S. T., and Kihara, D. Protein docking model evaluation by graph neural networks. *Frontiers in Molecular Biosciences*, 8:402, 2021.

Weiler, M., Geiger, M., Welling, M., Boomsma, W., and Cohen, T. 3d steerable cnns: Learning rotationally equivariant features in volumetric data. *arXiv preprint arXiv:1807.02547*, 2018.

Xu, K., Hu, W., Leskovec, J., and Jegelka, S. How powerful are graph neural networks? *arXiv preprint arXiv:1810.00826*, 2018.

Ying, R., You, J., Morris, C., Ren, X., Hamilton, W. L., and Leskovec, J. Hierarchical graph representation learning with differentiable pooling. *arXiv preprint arXiv:1806.08804*, 2018.

Zhang, J. and Zhang, Y. A novel side-chain orientation dependent potential derived from random-walk reference state for protein fold selection and structure prediction. *PloS one*, 5(10):e15386, 2010.

Zhemchuzhnikov, D., Igashov, I., and Grudinin, S. 6dcnn with roto-translational convolution filters for volumetric data processing. *arXiv preprint arXiv:2107.12078*, 2021.

## A. Proof of Rotation Equivariance

A function  $f$  taking a 3D vector  $\mathbf{x} \in \mathbb{R}^3$  as input is rotation equivariance, if applying ant rotation matrix  $\mathbf{R} \in \mathbb{R}^{3 \times 3}$  on  $\mathbf{x}$  leads to the same transformations of the output  $f(\mathbf{x})$ . Formally,  $f : \mathbb{R}^3 \rightarrow \mathbb{R}^3$  is rotation equivariance by fulfilling:

$$\mathbf{R}(f(\mathbf{x})) = f(\mathbf{R}\mathbf{x}) \quad (30)$$

For notation consistency, we consider each row of the matrix is an individual 3D vector and use right-hand matrix multiplication here. When performing equivariant message passing on protein graph for node  $i$  with local rotation matrix  $\mathbf{O}_i$ , we first transform the vector representations of its neighbors from global reference to its local reference, that is, for a particular neighbor node  $j$  with vector feature  $\mathbf{V}_j \in \mathbb{R}^{C \times 3}$ , apply our DWNN layers  $f$ , and transform the updated features back to the global reference. We set only one neighbor node  $u_j$  for  $u_i$  for simplicity. The updated vector representation  $\mathbf{V}_i$  for node  $i$  is

$$\mathbf{V}_i = [f(\mathbf{V}_j \mathbf{O}_i^T)] \mathbf{O}_i \quad (31)$$

If we apply a global rotation matrix  $\mathbf{R}$  to all vectors in the global frame, the local rotation matrix  $\mathbf{O}_i$  will be transformed to  $\mathbf{O}'_i = \mathbf{O}_i \mathbf{R}$ , and  $\mathbf{V}_j$  to be  $\mathbf{V}'_j = \mathbf{V}_j \mathbf{R}$ , now the output  $\mathbf{V}'_i$  is

$$\mathbf{V}'_i = [f(\mathbf{V}'_j \mathbf{O}'_i^T)] \mathbf{O}'_i \quad (32)$$

$$= [f(\mathbf{V}_j \mathbf{R} \mathbf{R}^T \mathbf{O}_i^T)] \mathbf{O}_i \mathbf{R} \quad (33)$$

$$= [f(\mathbf{V}_j \mathbf{O}_i^T)] \mathbf{O}_i \mathbf{R} \quad (34)$$

And if instead, we directly apply the rotation matrix to original output  $\mathbf{V}_i$ , we got

$$\mathbf{V}'_i = [f(\mathbf{V}_j \mathbf{O}_i^T)] \mathbf{O}_i \mathbf{R} \quad (35)$$

$$= \mathbf{V}_i \mathbf{R} \quad (36)$$

In other words, rotating the input leads to the same transformations to output, so we can preserve rotation equivariance for vector representations in this way. Note that scalar features remain invariant when applying global rotation, so our message-passing paradigm with global and local coordinate transformations is rotation equivariance.

## B. Experiment Details

We represent a protein 3D structure as an attributed graph, with each node and edge attached with scalar and vector features that are geometric-aware. We implement our DWNN in the equivariant message passing manner, with 3 layer Directed Weight Perceptrons for all tasks.

### B.1. Protein Features

In this paper, we use an attributed graph  $\mathcal{G} = (\mathcal{V}, \mathcal{E})$  to represent the protein structure, where each node corresponds to

one particular amino acid in the protein with edges connecting its k-nearest neighbors. Here we set  $k = 30$ . The node features  $\mathcal{V} = \{v_1, \dots, v_N\}$  and edge features  $\mathcal{E} = \{e_{ij}\}_{i \neq j}$  are both multi-channel scalar-vector tuples with scalar features like distances and dihedral angles and vector features like unit vectors representing particular orientations.

A node  $v_i$  represent the  $i$ -th residue in the protein with scalar and vector features describing its geometric and chemical properties if available. Therefore, a node in this graph may have multi-channel scalar-vector tuples  $(s_i, V_i)$ ,  $s_i \in \mathbb{R}^6$  or  $\mathbb{R}^{26}$ ,  $V_i \in \mathbb{R}^{3 \times 3}$  as its initial features.

- **Scalar Feature.** The  $\{\sin, \cos\} \circ \{\psi, \omega, \phi\}$ . Here  $\{\psi, \omega, \phi\}$  are dihedral angles computed from its four backbone atom positions,  $C\alpha_{i-1}, N_i, C\alpha_i, N_{i+1}$ .
- **Scalar Feature.** A one-hot representation of residue if the identity is available.
- **Vector Feature.** The unit vectors in the directions of  $C\alpha_{i+1} - C\alpha_i$  and  $C\alpha_{i-1} - C\alpha_i$ .
- **Vector Feature.** The unit vector in the direction of  $C\beta_i - C\alpha_i$  corresponds to the side-chain directions.

The edge  $e_{ij}$  connecting the  $i$ -th residue and the  $j$ -th residue also has multi-channel scalar-vector tuples as its feature  $(s_{ij}, V_{ij})$ ,  $s_{ij} \in \mathbb{R}^{34}$ ,  $V_{ij} \in \mathbb{R}^{1 \times 3}$

- **Scalar Feature.** The encoding of the distance  $\|C\alpha_j - C\alpha_i\|$  using 16 Gaussian radial basis functions with centers spaced between 0 to 20 angstroms.
- **Scalar Feature.** The positional encoding of  $j - i$  corresponding the relative position in the protein sequence.
- **Scalar Feature:** The contact signal describes if the two residues contact in the space, 1 if  $\|C\alpha_j - C\alpha_i\| \leq 8$  and 0 otherwise.
- **Scalar Feature.** The H-bond signal describes if there may be a H-bond between the two nodes calculated by backbone distance.
- **Vector Feature.** The unit vector in the direction of  $C\alpha_j - C\alpha_i$ .

## B.2. Model Details

**Synthetic Task.** We consider the length of each vector as one channel scalar feature  $\in \mathbb{R}$  and the vector itself as one channel vector feature  $\in \mathbb{R}^{1 \times 3}$ . The VNN and GVP models in this experiment are be set to 3 layers. And our DWP is only 1 layer. We also train a 3-layer MLP by concatenating the scalar and vector feature as a four-channel scalar feature

$\in \mathbb{R}^4$  as input. Specifically, the parameter counts of VNN, GVP, MLP, DWP is 24,28,24 and 24.

**CPD.** We train our model in a BERT-style recovery target (Strokach et al., 2020), more specifically, we dynamically mask 85% residues of the whole protein and let the model recover them using structure information from its neighbors using CrossEntropy loss. During testing, we mask all the residues and recover the whole protein sequence in one forward pass, we also try to iteratively predict one residue per forwarding pass.

**MQA.** Because MQA is a regression task, we train our model using MSE loss. When testing, we compute the different types of correlations between predicted scores and ground truth.

**RES.** Residue identity requires the model to classify the center residue from a local substructure of the protein. We construct a subgraph of each local substructure according to Section B.1. To guarantee equitable comparison, we retrain all the methods based on our protein graph from scratch.

**Fold and React.** For these two graph-level classification tasks, we construct graph for each protein as above and use CrossEntropy loss.

## B.3. Training Details

For the synthetic task, we train each model for 1000 epochs with a learning rate of  $1e - 3$  and plot the training loss for evaluation.

For all models we trained, we use 128 scalar channels and 32 vector channels for each node’s hidden representations, 64 scalar channels, and 16 vector channels for each edge’s hidden representations. We train our models with learning rate  $3e - 4$  for CPD and  $2e - 4$  for MQA,  $5e - 4$  for RES and  $1e - 3$  for REACT/FOLD, a dropout rate of 10% (Srivastava et al., 2014), and Layernorm paradigm. We train all the models on NVIDIA Tesla V100 for 100 epochs for each task.

## C. Ablation Studies

In the end, we conduct ablation experiments to study the contribution of different modules of our model on the tasks of CPD (table 1) and RES (table 2). More specifically, we replace the Directed Linear Module with the regular linear layer with scalar weights (No Directed Linear), remove the Interaction Module (No Interaction), and also break the equivariance by canceling coordinate transformations in the step of message passing (No Equivariance). As shown in Table 1, in general, all three components of our model are important since removing each of them results in a significant performance drop. According to the performance gain, the directed weights are the most important module for the CPD task. For Residue Identity, however, equivariance mes-

sage passing is the most important component, indicating that the necessity of rotation equivariance in learning the representation of local protein structures.

*Table 1.* Performance of different ablated CPD models on the CATH 4.2 and TS50 dataset.

Model	Perplexity ↓			Recovery % ↑			
	Short	Single-chain	All	Short	Single-chain	All	TS50
No DirectedLinear	6.52	6.79	5.28	36.7	35.0	42.9	46.8
No Interaction	6.45	6.36	4.87	37.2	36.3	44.9	48.7
No Equivariance	6.21	6.04	4.64	36.9	37.1	45.8	44.8
DW-GNN	<b>5.42</b>	<b>5.69</b>	<b>3.94</b>	<b>39.6</b>	<b>38.5</b>	<b>47.5</b>	<b>54.5</b>

*Table 2.* Performance of different ablated RES models on the ATOM3D dataset.

Model	No DirectedLinear	No Interaction	No Equivariance	DW-GNN
Acc %	47.3	47.7	33.0	<b>50.2</b>